A novel multi-waveband dispersion compensating fiber based on hybrid photonic crystal fiber*

LIU Ying(刘颖)[1,2]**, **LI Yu-quan**(李玉权)[1], **WANG Jing-yuan**(汪井源)[1], **XIE Xiao-gang**(谢晓刚)[1], and **LI Jian-hua**(李建华)[1]

1. Institute of Communications Engineering, PLA University of Science & Technology, Nanjing 210007, China

2. PLA Xi'an Communications Institute, Xi'an 710106, China

(Received 15 September 2012)

In view of dispersion compensating in multiple wavebands at the same time, this paper proposes a novel multi-waveband dispersion compensating fiber (DCF) based on hybrid photonic crystal fiber (PCF). The proposed fiber can compensate multiple wavebands at the same time. The mechanism of the multi-waveband dispersion compensation is analyzed, and the different material-filled structure is discussed numerically. The simulation results show that the multi-waveband DCF can compensate multiple wavelengths at the same time. By a reasonable design, this fiber can replace the multi-dispersion compensating system composed by cascaded multiple devices, and minimize the loads of the system in an efficient way.

Document code: A **Article ID:** 1673-1905(2013)01-0053-4

DOI 10.1007/s11801-013-2353-7

The control of chromatic dispersion is important for high-bit-rate communication system. In the recent years, photonic crystal fiber (PCF) has been well confirmed to have extraordinary specialties in controlling the chromatic dispersion[1-4]. The photonic crystal dispersion compensating fiber (DCF) is based on a dual-core structure of an inner concentric core and an outer ring core, which supports two supermodes, and could lead to a large negative dispersion by coupling these two modes[5-15]. Presently, the way for compensating the dispersion in optical communication system is to introduce dispersion compensating grating (DCG) or DCF with large negative dispersion on line. But these methods are for single propagation wavelength. In the wavelength division multiplexing (WDM) multi-wavelength system, all the working wavelengths need to be compensated at the same time. This makes the broadband and multi-wavelength dispersion compensating devices more popular. The multi-wavelength dispersion compensating methods often use wideband compensation DCG or DCF, or numbers of DCGs in cascade[16]. But these methods will increase the burden of the system, and introduce a waste of system resource. It is a very urgent need to use one device to compensate multiple wavelengths at the same time.

In view of this problem, this paper proposes a novel multi-waveband DCF based on hybrid PCF, which can compensate multiple wavebands at the same time. The proposed DCF has a hybrid lighting guide mechanism in the core region by selectively material-filling in different air holes. The proposed DCF can achieve a quite high negative dispersion coefficient, which is based on coupling between the hybrid guiding mode in the boundary of the band-gap in the core region and the index guiding mode in the cladding defect area. More importantly, the designed hybrid DCF possesses multiple band-gaps, so the couplings can happen in multiple wavelengths. So this hybrid DCF can get the multiple negative dispersion windows, which can compensate multiple wavelengths at the same time. Based on this extraordinary property, the designed DCF shows a big advantage compared with other ordinary DCFs.

Hybrid light guiding mechanism was firstly reported and manufactured by Cerqueira and his group[17,18]. They have proved that the light propagating along the fiber can be seen as index-guiding and band-gap guiding mechanisms, simul taneously. Based on the point, many works were concerned on hybrid PCFs[19-23]. In this paper, a hybrid structure around the core region is designed. Light propagating in the core region can be guided by both index-guiding mechanism and

* This work has been supported by the National Natural Science Foundation of China (No.61032005), and the Natural Science Foundation of Jiangsu Province in China (Nos.BK2011114 and BK2012509).

** E-mail:danfer_ice@163.com

band-gap guiding mechanism, and because of its special structure characteristics, it can get large negative dispersion in multiple wavebands. The schematic cross section of the designed hybrid DCF is shown in Fig.1. The air holes and the doped rods in the hybrid DCF are arranged in a hexagonal pattern, with a pitch Λ of 7.5 μm. The central defect core is the positively doped region with the refractive index of 1.451 and the diameter d_1 of 6 μm. The other four positively doped rods with the refractive index of 1.490 and the diameter d_2 of 3 μm are distributed in x and y directions, respectively, for different structures of A and B. The diameter of all the other air holes is also d_2=3 μm, and the background index is 1.450.

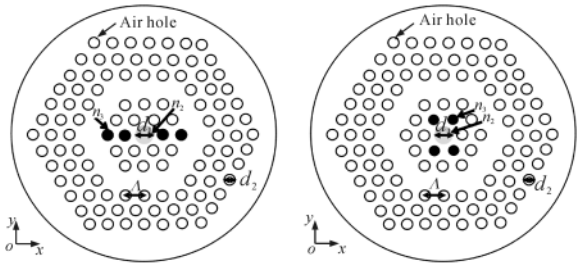

(a) Structure A (b) Structure B

Fig.1 Schematic cross sections of the designed hybrid DCFs

Taking structure B as example, owing to that the refractive index of the core is higher than that of the cladding along the x direction, the propagation light confined in the core in the same direction can be guided by total internal reflection, which is so called index-guiding mechanism. On the other hand, the refractive index of cladding rods along the y direction is higher than that of the doped core region. The propagating light in this direction can be only guided by the photonic band-gap effect. So the light confined in the core region is guided by both index-guiding mechanism and band-gap guiding mechanism. The guide mechanism in structure A is the same as that in structure B, and only the index guiding direction and band-gap guiding direction are opposite. When the propagating wavelengths are set within the band-gaps, the guiding mode in the core region is guided by both index-guiding and band-gap guiding mechanisms. But near the boundary of the band-gaps, the confinement ability of band-gap to the guiding mode becomes weak, so the mode confined in the core field can leakage gradually to the cladding defect area of the fiber. Then the coupling between the guiding mode in the boundary of the band-gap and the cladding defect mode occurs. And then, there will be a very large negative dispersion. For the proposed DCF, the multi-waveband structure and the special dispersion compensating mechanism make the coupling between the hybrid core mode and the cladding defect mode occur for several times. This extraordinary property makes the proposed DCF have a big advantage over other ordinary DCFs. The dispersion compensation mechanism is shown in Fig.2.

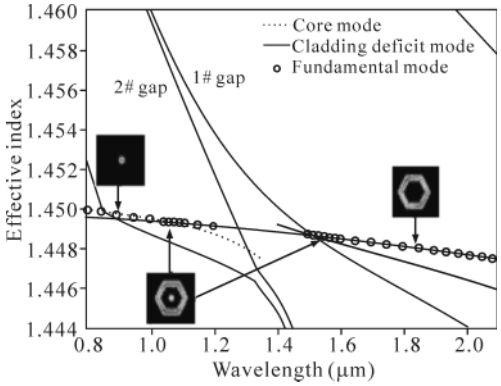

Fig.2 Effective refractive index and band-gaps of the designed hybrid DCF as a function of wavelength and the mode field distributions

Fig.2 shows the effective refractive index and the band-gaps of the designed hybrid DCF as a function of wavelength. In Fig.2, the circled line results from the combined effect of the core mode index and the cladding mode index, which denotes the combined fundamental mode of the hybrid DCF. At the phase matching wavelength $\ddot{e}_p$, the combined effective index shows a kink near the boundary of each band-gap. It is because the confinement ability of band-gap to the guiding mode here is weaker than that in the middle of the band-gap, and the guiding mode in the boundary of the band-gap suddenly moves to the cladding defect field. The distributions of the guiding modes when $\ddot{e}<\ddot{e}_p$, $\ddot{e}=\ddot{e}_p$ and $\ddot{e}>\ddot{e}_p$ are also shown in Fig.2, respectively. When $\ddot{e}<\ddot{e}_p$, the mode field is tightly confined in the core field, and it is a hybrid guiding mode of index-guiding and band-gap guiding mechanisms. When the wavelength is near the phase matching wavelength $\ddot{e}_p$, the mode confined in the core field leakages gradually to the cladding defect area of the fiber. It is because of the weakening of the confinement ability of band-gap to the guiding mode. When $\ddot{e}>\ddot{e}_p$, the distribution of the mode field is mainly in the cladding defect area. As mentioned before, coupling between the guiding mode in the boundary of the band-gap and the cladding defect occurs around the phase matching wavelength $\ddot{e}_p$, so that a large negative dispersion appears.

All the numerical analyses are solved by plane wave expansion (PWE) method and the full-vector finite element method (FEM) with anisotropic perfectly matched layers (PMLs). The eigenvalue and the band-gap map can be calculated by PWE. With the help of the FEM with PML, the wavelength dependence of the effective index n_{eff} and other properties of the fiber, such as the dispersion D, can be easily calculated.

The chromatic dispersion can be directly calculated when the mode effective index n_{eff} as a function of the wavelength λ is determined, and the chromatic dispersion D of the DCF can be obtained from[24]

$$D = -\frac{\lambda}{c}\frac{\mathrm{d}^2 \operatorname{Re}(n_{\text{eff}})}{\mathrm{d}\lambda^2} , \quad (1)$$

where n_{eff} is the mode effective index, c is the velocity of light in vacuum, and Re(·) stands for the real part of the physical quantity.

Our previous work[25] has discussed the effects of the geometric parameters on the properties of the DCF already. So now the effect of the distribution of the positively doped rods on the properties of the DCF is discussed. Due to the variations of the two orthogonal fundamental modes are similar, only the *y*-polarized fundamental mode in our simulations is considered.

Fig.3 shows the mode effective index curves of the proposed DCF for different structures A and B. We can see from Fig.3 that there are two transitions for the curve around 1.08 ìm and 1.47 μm for structure A, and for structure B, the transitions are shown around 1.07 μm and 1.53 μm. This is because the guiding mode in the edge of the band-gap transports quickly to the cladding defect area. From Fig.3 we can see that for the band-gap guiding mode in the core region, the mode effective index curves of the two different structures almost coincide with each other before the coupling occurs. This is because the band-gap maps of structures A and B are the same, and the mode effective indices of the band-gap guiding modes are similar. The little difference is caused by the different distributions of the high index rods, which makes the hybrid guiding modes in two different structures different from each other. The change of the transition wavelength for fundamental mode is caused by the different distributions which affect the coupling efficiency. The coupling of the two modes for a dual-core structure PCF is affected by the first ring of the air holes[13]. For our case, the high index rods in the first ring of the air holes in structure B are more than those in structure A, so the confinement ability of band-gap to the guiding mode in structure B is stronger than that in structure A. That is to say, during the coupling of the guiding mode in the boundary of the band-gap and the cladding defect mode, the power exchange in structure B is more than that in structure A. The difference leads to the change of the index curve transition and the increase of the value of the negative dispersion. The increase of the dispersion is shown in Fig.4. For Fig.3, the effective index curves for different structures after the transition almost coincide with each other. This is because the dominant guiding mode in the fiber is the index-guiding mode after the coupling occurs. The cladding structures for A and B are the same with each other, so the index curves almost coincide with each other.

Fig.4 shows the chromatic dispersion curves for different structures. It can be seen that the dispersion in structure B is larger than that in structure A. This is because more power is transferred from the band-gap guiding mode to the cladding defect mode in structure B. The dispersion for structure B is -350 ps/(nm • km) around 1.07 μm, and -760 ps/(nm • km) around 1.53 μm. The dispersion for structure A is -210 ps/(nm • km) around 1.08 μm, and -435 ps/(nm • km) around 1.47 μm. According to the numerical analyses above, we should adopt structure B in design to get larger negative dispersion. It can decrease the loss and fibers in compensating. Then, we can implement multi-waveband dispersion compensation in one device by reasonable design.

For dispersion compensating in multiple wavebands at the same time, a novel multi-waveband DCF based on hybrid PCF is proposed. The numerical results show that the proposed DCF has a hybrid lighting guide mechanism in the core region by selectively material-filling in different air holes. And by a reasonable design, the proposed DCF can realize the coupling of the hybrid guiding mode in the boundary of the band-gaps to get large negative dispersion in multiple wavebands. This outstanding property can be useful in

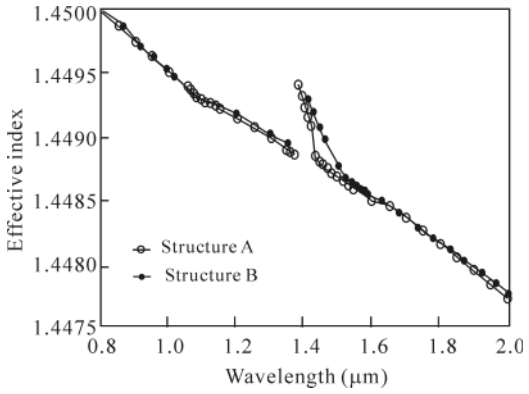

Fig.3 Mode effective index curves of the proposed DCF for structures A and B

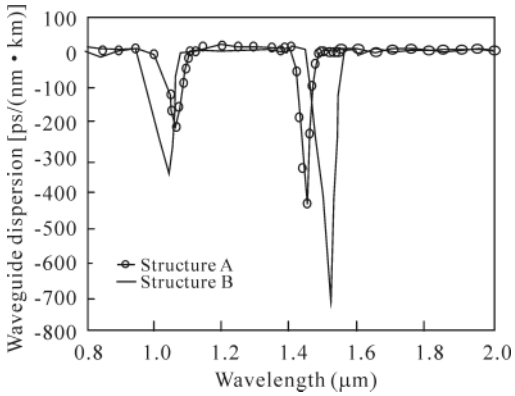

Fig.4 Chromatic dispersion versus wavelength for different structures

multi-waveband dispersion compensating system to replace the method using numbers of DCGs in cascade, and to reduce the burden and resource wasting of the system.

References

[1] K. Thyagarajan, R. K. Varshney, P. Palai, A. K. Ghatak and L. C. Goyal, IEEE Photon. Technol. Lett. **8**, 1510 (1996).

[2] Jingyuan Wang, Chun Jang, Weisheng Hu and Mingyi Gao, Opt. Laser Technol. **38**, 169 (2006).

[3] T. J. Yang, L. F. Shen, Y. F. Chau, M. J. Sung, D. Chen and D. P. Tsai, Opt. Commun. **281**, 4334 (2008).

[4] J. H. Liou, S. S. Huang and C. P. Yu, Opt. Commun. **283**, 971 (2010).

[5] J. L. Auguste, R. Jindal, J. M. Blondy, M. Clapeau, J. Marcou, B. Dussardier, G. Monnom, D. B. Ostrowsky, B. P. Pal and K. Thygarajan, Electron. Lett. **36**, 1689 (2000).

[6] F. Gérôme, J.-L.Auguste and J.-M. Blondy, Optics Lett. **29**, 2725 (2004).

[7] Yi Ni, Lei Zhang, Liang An, Jiangde Peng and Chongcheng Fan, IEEE Photon. Technol. Lett. **16**, 1516 (2004).

[8] A. Huttunen, Opt. Express **13**, 627 (2005).

[9] Zhihua Zhang, Yifei Shi, Baomin Bian and Jian Ju, IEEE Photon. Technol. Lett. **20**, 1402 (2008).

[10] Wang Honghua, Xue Wenrui and Zhang Wenmei, Acta Optica Sinica **28**, 27 (2008). (in Chinese)

[11] Ming Chen, Qing Yang, Tiansong Li, Mingsong Chen and Ning He, Opt. Int. J. Light Electron. Opt. **121**, 867 (2010).

[12] Han Jiawei and Hou Shanglin, Slope-Matching Profile Optimization of Dual-Concentric-Core Photonic Crystal Fiber for Broadband Dispersion Compensation, ACP, Shang Hai, 1 (2009).

[13] Soan Kim and Chul-Sik Kee, Opt. Express **17**, 15885 (2009).

[14] Maggie Yihong Chen, Harish Subaraman and Ray T. Chen, Dual-Concentric-Core Photonic Crystal Fiber with -5400 ps/nm/km Dispersion Coefficient, OSA/OFC/NFOEC, 2009.

[15] Aliramezani M. and Mohammad Nejad Sh., Opt. Laser Technol. **42**, 1209 (2010).

[16] Yu Wenke, Lou Caiyun, Zhao Xiaofan, Lu Dan and Chen Jianhua, Acta Optica Sinica **31**, 30 (2011). (in Chinese)

[17] Arismar Cerqueira S. Jr., F. Luan, C. M. B. Cordeiro, A. K. George and J. C. Knight, Design and Fabrication of Hybrid Photonic Crystal Fibers, CLEO/QELS Conference, 1 (2006).

[18] Arismar Cerqueira S. Jr., F. Luan, C. M. B. Cordeiro, A. K. George and J. C. Knight, Opt. Express **14**, 926 (2006).

[19] Mathias Perrin, Yves Quiquempois, G'eraud Bouwmans and M.Douay, Opt. Express **15**, 13783 (2007).

[20] Limin Xiao, Wei Jin and M. S. Demokan, Opt. Express **15**, 15637 (2007).

[21] J. Sun and C. C. Chan, J. Opt. Soc. Am. B. **24**, 2640 (2007).

[22] Xiao-Hui Fang, Ming-Lie Hu, Yan-Feng Li, Lu Chai, Ching-Yue Wang and Aleksei M. Zheltikov, Opt. Lett. **35**, 493 (2010).

[23] Nicolai Granzow, Patrick Uebel, Markus A. Schmidt, Andrey S. Tverjanovich, Lothar Wondraczek and Philip St. J. Russell, Opt. Lett. **36**, 2432 (2011).

[24] Saitoh. Kunimasa and Koshiba. Masanori, Optics Express **11**, 3100 (2003).

[25] Ying Liu, Yuquan Li, Jingyuan Wang, Rong Wang, Jianhua Li and Xiaogang Xie, Optics & Laser Technology **44**, 2076 (2012).